International Journal of Materials Science and Applications
2014; 3(5): 274-278
Published online September 30, 2014 (http://www.sciencepublishinggroup.com/j/ijmsa)
doi: 10.11648/j.ijmsa.20140305.30
ISSN: 2327-2635 (Print); ISSN: 2327-2643 (Online)

A theoretical study of the heavy and light hole properties of $Cd_{1-x}Zn_xS$ quantum dot superlattices

Saber Marzougui, Nabil Safta*

Unité de Physique Quantique, Faculté des Sciences, Université de Monastir, Monastir, Tunisia

Email address:
saftanabil@yahoo.fr (N. Safta)

To cite this article:
Saber Marzougui, Nabil Safta. A Theoretical Study of the Heavy and Light Hole Properties of $Cd_{1-x}Zn_xS$ Quantum Dot Superlattices. *International Journal of Materials Science and Applications.* Vol. 3, No. 5, 2014, pp. 274-278. doi: 10.11648/j.ijmsa.20140305.30

Abstract: This work reports on a theoretical investigation of superlattices based on $Cd_{1-x}Zn_xS$ quantum dots embedded in an insulating material. This system, considered as a series of flattened cylindrical quantum dots with a finite barrier at the boundary, is studied using the tight binding approximation. The ground miniband width and the longitudinal effective mass, in the case of the heavy and light holes, have been computed as a function of zinc composition for different inter-quantum dot separations. An analysis of the results shows that the Zn composition x = 0.8 are appropriate to give rise a superlattice behavior for the light holes. As for the heavy holes, it has been showed the strong localization character of theses carriers in the $Cd_{1-x}Zn_xS$ nanostructures.

Keywords: Quantum Dots, Superlattices, $Cd_{1-x}Zn_xS$, Heavy and Light Holes, Tight Binding Approximation, Specific Devices

1. Introduction

In the last decades, films of $Cd_{1-x}Zn_xS$ have found wide applications in electrical, optical and electro – optical devices [1-3].The high potentialities of these films is mainly due to their utility as window materials in heterojunction solar cells with a p-type absorber like $CuInSe_2$, $CuIn_xGa_{1-x}Se_2$ or $CuSnS_z$ Se_{1-z} [4-6]. On the other hand, $Cd_{1-x}Zn_xS$ thin films have led to a decrease in window absorption and to an increase in the short circuit current as well [7-9].

To the subject of $Cd_{1-x}Zn_xS$ quantum dots (QDs), their considerable interest has been proved in both fundamental and applied research [4, 10-20]. For our part, we have adopted, in a first time, the spherical geometry with a finite potential barrier at the boundary to describe the $Cd_{1-x}Zn_xS$ QDs [21, 22]. Thus, by restricting the study to the ground state for both electrons and holes, we have calculated, in a first step, the shape of the confinement potentials, the quantized energies, their related envelope wave – functions and the QDs sizes [21]. We have calculated, in a second step, for electrons and holes, the excited bound states [22]. All these calculations have been made versus the zinc composition.

We have suggested, in a second time, the flattened cylindrical geometry with a finite potential barrier at the boundary [23-29]. Using this model, we have investigated, in a first step, the electronic properties of $Cd_{1-x}Zn_xS$ quantum dots [23]. More precisely, we have calculated the shape of the confining potential, the subband energies and their eigen envelope wave functions. We have studied, in a second step, the coupling in the case of superlattices based on $Cd_{1-x}Zn_xS$ quantum dots embedded in an insulating material with use of several potential models and different methods (Kronig – Penney method, sinusoidal and triangular potentials, Tight Binding approximation…) [24-29]. In this context, our interest has been focused, in a recent study, on the computation of the ground miniband width and the longitudinal effective mass for the electrons. Calculations have been made versus the ZnS molar fraction for different superlattice periods with use of the Tight Binding approximation (TBA) [28]. From this study, we have deduced that the Zn compositions x = 0.4 and x = 0.6 are appropriate to give rise a superlattice behavior for conduction electrons. As for the longitudinal electron effective mass, it is found to be the lower for x = 0.4 and x = 0.6 [28].

The goal of the present work is to extend the last study to the heavy and light holes. The paper is organized as follows: after a brief introduction, we present the theoretical details, the numerical results and discussions. The conclusions are

presented in the last part.

2. Theoretical Details

Fig. 1- a depicts the geometry used to describe a chain of $Cd_{1-x}Zn_xS$ QDs. The common confined direction is denoted by z. The inter-quantum dot separation is labelled d which corresponds to the period of the structure. Along a common direction of spherical $Cd_{1-x}Zn_xS$ QDs, electrons and holes see a succession of flattened cylinders of radius R and effective height L. If we consider L = 1 nm [23] and the fact that the diameter D = 2R varies from 9 nm to 4 nm going from CdS to ZnS [4] it clearly appears that L is lower than D. Consequently the quantum confinement along transversal direction can be disregarded and the $Cd_{1-x}Zn_xS$ multi – quantum dot system being studied can be considered as a QDs superlattice along the longitudinal confined direction. Thus, the system to investigate is a $Cd_{1-x}Zn_xS$ QD superlattice where the $Cd_{1-x}Zn_xS$ flattened cylinders QDs correspond to wells while the host dielectric lattice behaves as a barrier of height U_0. For the sake of simplicity, the electron and hole states are assumed to be uncorrelated. The problem to solve is, then, reduced to those of one particle in a one dimensional potential. In this work, we consider the potential depicted in Fig. 1- b. Such a potential can be expressed as:

$$V_{e,h}(z) = \sum_n U_{e,h}(z - nd) \tag{1}$$

with

$$U_{e,h}(z) = \begin{cases} -U_{0e,h}; & -L/2<z<L/2 \\ 0 \quad\quad ; & L/2<z<d-L/2 \end{cases}$$

The subscripts e and h refer to electrons and holes respectively and n is the nth period. For this potential, the electron and hole states can be calculated using the effective Hamiltonian:

$$H_{e,h} = \frac{-\hbar^2}{2m^*_{e,h}}\frac{d^2}{dz^2_{e,h}} + V_{e,h}(z_{e,h}) \tag{2}$$

where $\hbar$ is the Plank's constant and m^* is the effective mass of carriers. In deriving the Hamiltonian $H_{e,h}$, we have adopted the effective mass theory (EMT) and the band parabolicity approximation (BPA). The difference of the effective mass between the well and the barrier has been neglected.

We have resolved the Schrodinger equation using the Tight Binding Approximation. A peculiar attention is paid to the longitudinal dispersion relation which shows the k-dependence of minibands along the [001] direction. If we neglect the wave function overlap, this relation is given, in the case of the ground miniband (Γ_1 – miniband), by [28]:

$$E_{e,h}(k_z) = (E_{1e,h} - U_{0e,h}) + 2\gamma_{e,h} + 2\beta_{e,h}\cos(k_z d) \tag{3}$$

Here, E_{1e} corresponds to the lowest energy of electrons and E_{1h} is the lowest energy of holes ($E_{1h} \equiv E_{1hh}$ for heavy holes and $E_{1h} \equiv E_{1lh}$ for light holes). All these energies are associated with an isolated flattened cylindrical quantum dot of $Cd_{1-x}Zn_xS$ and calculated in such a way that the zero energy is taken at the bottom of the QD well [23, 29].

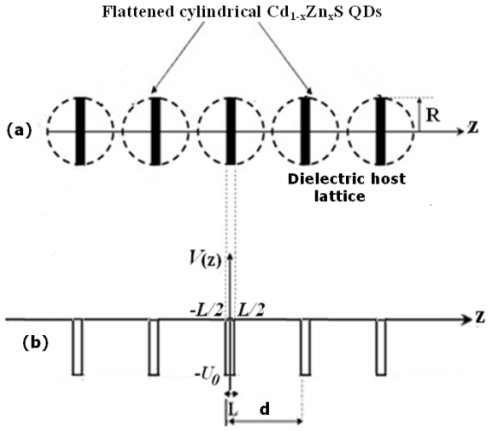

Figure 1. *(a) A schematic diagram of $Cd_{1-x}Zn_xS$ QD superlattices according to the flattened cylindrical geometry – (b) The barrier potential in the framework of the Tight Binding Approximation.*

β_e and γ_e are respectively, the exchange and the correlation integrals. These parameters are, respectively, given by:

$$\beta_{e,h} = -\frac{2U_{0e,h}A_{e,h}B_{e,h}e^{-\rho_{e,h}\left(d-\frac{L}{2}\right)}}{\rho_{e,h}^2 + k_{e,h}^2}\left(\rho_{e,h}\cos\left(\frac{k_{e,h}L}{2}\right)sh\left(\frac{\rho_{e,h}L}{2}\right) + k_{e,h}\sin\left(\frac{k_{e,h}L}{2}\right)ch\left(\frac{\rho_{e,h}L}{2}\right)\right)$$

$$\gamma_{e,h} = -\frac{U_{0e,h}B_{e,h}^2 e^{\rho_{e,h}(L-2d)}}{\rho_{e,h}}sh\left(\frac{\rho_{e,h}L}{2}\right)$$

with

$$A_{e,h} = \left[\frac{L}{2} + \frac{\cos^2\left(\frac{k_{e,h}L}{2}\right)}{\rho_{e,h}} + \frac{\sin(k_{e,h}L)}{2k_{e,h}}\right]^{-\frac{1}{2}}$$

$$B_{e,h} = A_{e,h}\cos\left(\frac{k_{e,h}L}{2}\right)$$

$$k_{e,h} = \sqrt{\frac{2m^*_{e,h}E_{1e,h}}{\hbar^2}}; \quad \rho_{e,h} = \sqrt{\frac{2m^*_{e,h}(U_{0e,h} - E_{1e,h})}{\hbar^2}}$$

3. Results and Discussion

We have computed, for the heavy and light holes, the longitudinal dispersion relation of the Γ_1 – miniband, given by Eq. (3), as a function of the ZnS molar fraction, for superlattice periods going from d = 1.5 nm to d= 2.5 nm. Values of parameters used in this computation are

summarized in Table 1. All these parameters are taken from Refs [23, 29]. Values of the effective masses of the heavy and light holes for $Cd_{1-x}Zn_xS$ with different Zn compositions have been deduced using the Vegard's law.

Table 1. *Parameters used to calculate the Γ_1 - miniband in the case of the heavy and light holes for $Cd_{1-x}Zn_xS$ QD superlattices.*

x	$\frac{m^*_{hh}}{m_0}$	$\frac{m^*_{lh}}{m_0}$	U_{0h}(eV)	L(nm)	E_{1hh}(eV)	E_{1lh}(eV)
0.0	5.00	0.70	0.25	1.00	0.040	0.129
0.2			0.25	1.00	0.049	0.136
0.4			0.50	1.00	0.060	0.216
0.6			0.50	1.00	0.070	0.238
0.8			0.50	1.00	0.083	0.266
1.0	1.76	0.23	2.00	1.00	0.145	0.538

One can easily deduce, from (3), that the Γ_{1h} - miniband width is given by:

$$\Delta E_{1h} = 4\left|\beta_h\right| \tag{4}$$

Thus, we have carried out this parameter for all the compositions and superlattice periods studied. Typical results are reported in Table 2 and Table 3.

Table 2. *The Γ_1 - miniband width (10^{-3} eV), as calculated for the heavy holes versus the ZnS molar fraction for different inter-QD separations.*

d (nm)	1.5	1.7	1.9	2.1	2.3	2.5
x						
0.2	7.628	3.059	1.174	4.507	0. 173	0. 066
0.4	3.596	0.973	0.263	0.071	0. 193	0. 005
0.6	6.533	2.020	6.248	0. 193	0. 059	0. 018
0.8	16.31	4.312	1.546	0. 554	0. 198	0. 071
1.0	1.887	0.029	0. 046	0. 037	0. 001	0. 002

This study led, for the light holes, to several observations: (i) ΔE_{1lh} shows a decreasing tendency when d increases independently of the Zn composition. As a consequence, the coupling decreases as the inter – quantum dot separation increases (ii) for $Cd_{1-x}Zn_xS$ QDs with x = 0; 0.2 and 0.4, ΔE_{1lh} is globally low (iii) for ZnS QD superlattices, ΔE_{1lh} shows a drastic drop as the inter – quantum dot separation increases. Thus, the coupling is very weak at high SL periods. In this case, $Cd_{1-x}Zn_xS$ nanocrystallites are nearly isolated (iv) for x = 0.8, ΔE_{1lh} is maximum independently of the inter-quantum dot separation. This reflects the strong degree of coupling between the QDs. Since the well width L being the same for all Zn compositions, these results are, most probably, related to the barrier potential height U_{0h}, the bulk effective mass m^*_{lh} and the energy E_{1lh} values (v) For $Cd_{1-x}Zn_xS$ QDs with x = 0.6, the magnitude order of ΔE_{1lh} is not far from the one of x = 0.8.

The comparison with results obtained for electrons [28] shows that ΔE_{1lh} is, globally, slightly lower than the Γ_1 - miniband width for electrons (Table 4). Therefore, the superlattice behavior affects not only the conduction electrons but also the light holes especially for short SL periods.

As for the heavy holes, ΔE_{1hh} is insignificant in terms of magnitude order which means that the strong localization character of heavy holes in the SL systems is totally preserved going from CdS to ZnS independently to the SL periods. As a consequence, we can consider that there is no formation of minibands.

Table 3. *The Γ_1 - miniband width (eV), as calculated for the light holes versus the ZnS molar fraction for different inter-QD separations.*

d (nm)	1.5	1.7	1.9	2.1	2.3	2.5
x						
0.2	0.190	0.115	0.088	0.067	0.053	0. 039
0.4	0.187	0.126	0.085	0.058	0. 039	0. 026
0.6	0.236	0.174	0.117	0. 083	0. 059	0. 042
0.8	0.313	0.217	0.164	0. 123	0. 091	0. 070
1.0	0.301	0.173	0.095	0. 052	0. 029	0. 016

Table 4. *The Γ_1 - miniband width, as calculated for electrons versus the ZnS molar fraction for different inter-QD separations[28].*

d (nm)	1.5	1.7	1.9	2.1	2.3	2.5
x						
0.0	0.056	0.054	0.052	0.050	0.048	0.046
0.2	0.211	0.189	0.169	0.151	0.135	0.121
0.4	0.352	0.294	0.242	0.201	0.167	0.139
0.6	0.406	0.302	0.224	0.166	0.123	0.091
0.8	0.344	0.208	0.125	0.076	0.045	0.027
1.0	0.241	0.126	0.065	0.034	0.017	0.009

Concerning the longitudinal effective mass of light holes m^*_{lh,Γ_1}, we can write [28]:

$$m^*_{lh,\Gamma_1} = \frac{\hbar^2}{2\left|\beta_{lh}\right|d^2} \tag{5}$$

We have calculated this parameter, in the case of the light holes, versus composition x for the different inter – QD separations studied. All these effective masses are expressed in units of the free electron mass m_0. Results are reported in Table 5.

Table 5. *The longitudinal effective mass calculated, for the light holes, as a function of the inter-sheet separation for $Cd_{1-x}Zn_xS$ QD superlattices*

d(nm)	1.5	1.7	1.9	2.1	2.3	2.5
x						
0.2	0.446	0.457	0.499	0.519	0.563	0.619
0.4	0.362	0.407	0.493	0.597	0.734	0.920
0.6	0.287	0.299	0.359	0.413	0.470	0.556
0.8	0.216	0.242	0.257	0.277	0.305	0.346
1.0	0.223	0.308	0.444	0.655	1.066	1.518

An analysis of the obtained results revealed: (i) m^*_{lh,Γ_1} shows an increasing tendency when d increases independently of the Zn composition. Therefore, the light hole mobility is expected to be decreasing with increased d (ii) for $Cd_{1-x}Zn_xS$ QDs with x = 0; 0.2 and 0.4, m^*_{lh,Γ_1} values are globally high (iii) for ZnS QD superlattices, m^*_{lh,Γ_1} values are rather high for large SL periods. In this case, the transport of light holes is significantly reduced (iv) for x = 0.8, the order of magnitude of m^*_{lh,Γ_1} is low independently of the inter-quantum dot separation. It is of particular interest that, for this composition, the SL period does not significantly affect the transport properties (v) For $Cd_{1-x}Zn_xS$ QDs with x = 0.6, m^*_{lh,Γ_1} is slightly higher than the one of x = 0.8.

It should be noted that, for the heavy holes, the $Cd_{1-x}Zn_xS$ nanoparticles behave as isolated QDs. The effective mass being related to the miniband dispersion can not be defined in such a case.

4. Conclusion

We investigated the coupling in superlattices made by $Cd_{1-x}Zn_xS$ QDs for compositions ranging from CdS to ZnS. To describe the QDs, we have proposed the flattened cylindrical geometry with a finite potential barrier at the boundary. Using the Tight Binding Approximation, we have calculated, in a first step, for the heavy and light holes the Γ_1 - miniband. Calculations have been made as a function of Zn composition for different inter – quantum dot separations.

An analysis of the obtained results has evidenced that the Zn composition x = 0.8 are appropriate to give rise a superlattice behavior for the light holes. As for the heavy holes, the results showed the strong localization character of theses carriers in the $Cd_{1-x}Zn_xS$ nanostructures. Concerning the longitudinal effective mass of the light holes, it is found to be the lower for x = 0.8.

In the applied physics, this study open a new way for designing specific devices based on well controlled $Cd_{1-x}Zn_xS$ QDs especially the non – volatile memories.

References

[1] A. Sakly, N. Safta and A. Ben Lamine. (2004), Interpretation of the bowing phenomenon in $Cd_{1-x}Zn_xS$ alloy, J. Mater. Sci.-Mater. Electron. 15 : 351.

[2] N. A. Shah, A. Nazir, W. Mahmood, W. A. Syed, S. Butt, Z. Ali and A. Maqsood. (2012), Physical properties and characterization of Ag doped CdS thin films, J. Alloys Compd. 512: 27.

[3] T. P. Kumar, S. Saravanakumar and K. Sankaranayanan. (2011), Effect of annealing on the surface and band gap alignment of CdZnS thin films, Appl. Surf. Sci. 257 (6) : 1923.

[4] B. Bhattacharjee, S. K. Mandal, K. Chakrabarti, D. Ganguli and S. Chaudhui. (2002), Optical properties of Cd1−xZnxS nanocrystallites in sol–gel silica matrix, J. Phys. D: Appl. Phys. 35: 2636-2642.

[5] H. H. Gürel, Ö. Akinci and H. Ünlü. (2008), Tight binding modeling of CdSe/ZnS and CdZnS/CdS II–VI heterostructures for solar cells: Role of d-orbitals, Thin Solid Films 516 : 7098.

[6] M. Gunasekaram, M. Ichimura. (2007), Photovoltaic cells based on pulsed electrochemically deposited SnS and photochemically deposited CdS and Cd1−xZnxS, Sol. Energy Mater. Sol. Cells. 91 : 774.

[7] N. Kohara, T. Negami, M. Nishitani and T. Wada. (1995), Preparation of Device – Quality Cu (In, Ga)Se_2 Thin films deposited by Coevaporation with composition Monitor, Japan. J. appl. Phys. 34 : L 1141

[8] V. Alberts, R. herberhonz, T. Walter and H. W. Schock. (1997), Device characteristics of In-rich $CuInSe_2$ based solar cells, J. Phys. D: Appl. Phys. 30 : 2156.

[9] J. Lee, W. Song and J. Yi. (2003), Growth and properties of the $Cd_{1-x}Zn_xS$ films for solar cell applications, Thin Solid Films 431-432 : 349.

[10] A. J. Peter and C. W. Lee.(2012), Electronic and optical properties of CdS/CdZnS nanocrystals, Chinese Phys. B 21: 087302.

[11] F. Scotognella, G. Lanzani, L. Manna, F. Tassone and M. Zavelani-Rossi. (2012), Study of higher-energy core states in CdSe/CdS octapod nanocrystals by ultrafast spectroscopy, Eur. Phys. J. B. 85: 128.

[12] L. Cao, S. Huang and S. E. (2004), ZnS/CdS/ZnS quantum dot quantum well produced in inverted micelles, J. colloid Interface Sci. 273: 478-482.

[13] H. Kumano, A. Ueta and I. Suemune. (2002), Modified spontaneous emission properties of CdS quantum dots embedded in novel three-dimensional microcavities, Physica E 13: 441-445

[14] Y. C. Zhang, W. W. Chen and X. Y. Hu. (2007), In air synthesis of hexagonal $Cd_{1-x}Zn_xS$ nanoparticles from single-source molecular precursors, Mater. Lett. 61: 4847-4850

[15] C. S. Pathak, D. D. Mishra, V. Agarawala, M. K. Mandal. (2012), Mechanochemical synthesis, characterization and optical properties of zinc sulphide nanoparticles, Indian J. Phys 86: 777-781.

[16] S. Roy, A. Gogoi and G. A. Ahmed. (2010), Size dependent optical characterization of semiconductor particle: CdS embedded in polymer matrix, Indian J. Phys. 84: 1405-1411

[17] A. U. Ubale and A. N. Bargal. (2010), Characterization of nanostructured photosensitive cadmium sulphide thin films grown by SILAR deposition technique, Indian J. Phys. 84: 1497-1507

[18] K.K Nanda, S.N. Sarangi, S. Mohanty, S.N. Sahu. (1998), Optical properties of CdS nanocrystalline films prepared by a precipitation technique, Thin Solid Films 322: 21-27.

[19] N. Safta. (2004), Fluctuations mode of the gap as a function of composition of Cd1-xZnxS ternaries, Ann. Chim. Sci. Mat. 29 (5) 105-112

[20] H. Yükselici, P. D. Persans and T. M. Hayes.(1995), Optical studies of the growth of Cd1-*x*Zn*x*S nanocrystals in borosilicate glass, Phys. Rev. B. 52: 11763.

[21] N. Safta, A. Sakly, H. Mejri and Y. Bouazra. (2006), Electronic and optical properties of $Cd_{1-x}Zn_xS$ nanocrystals, Eur. Phys. J. B 51: 75-78

[22] A. Sakly, N. Safta, A. Mejri, H. Mejri, A. Ben Lamine. (2010), The Excited Electronic States Calculated for Cd1-*x*Zn*x*S Quantum Dots Grown by the Sol-Gel Technique, J. Nanomater, ID746520.

[23] N. Safta, A. Sakly, H. Mejri and M. A. Zaïdi. (2006), Electronic properties of multi-quantum dot structures in $Cd_{1-x}Zn_xS$ alloy semiconductors, Eur. Phys. J. B 53: 35 – 38

[24] A. Sakly, N. Safta, H. Mejri, A. Ben Lamine. (2009), The electronic band parameters calculated by the Kronig–Penney method for Cd_{1-}xZnxS quantum dot superlattices, J. Alloys Compd. 476: 648–652.

[25] A. Sakly, N. Safta, H. Mejri, A. Ben Lamine. (2011), The electronic states calculated using the sinusoidal potential for Cd_{1-}xZnxS quantum dot superlattices, J. Alloys Compd.509: 2493–2495

[26] S. Marzougui, N. Safta. (2014), The electronic band parameters calculated by the Triangular potential model for $Cd_{1-x}Zn_xS$ quantum dot superlattices, IOSR-JAP 5 (5) : 36-42

[27] S. Marzougui, N. Safta. (2014), The electronic band parameters calculated by the Tight Binding Approximation for $Cd_{1-x}Zn_xS$ quantum dot superlattices, IOSR-JAP 6 (2) : 15-21

[28] S. Marzougui, N. Safta. (2014), A theoretical study of the electronic properties of $Cd_{1-x}Zn_xS$ quantum dot superlattices, *American Journal of Nanoscience and Nanotechnology* 2 (3) : 45-49.

[29] S. Marzougui. (2011), *A study of the excited states in the flattened cylindrical quantum dots of* $Cd_{1-x}Zn_xS$, Master, University of Monastir.